Theodore H. H. Pian
Massachusetts Institute of Technology
Cambridge, Massachusetts 02139

ABSTRACT

The paper describes a procedure for modelling the anisotropic elastic-plastic behavior of metals in plane stress state by the mechanical sub-layer model. In this model the stress-strain curves along the longitudinal and transverse directions are represented by short smooth segments which are considered as piecewise linear for simplicity. The model is incorporated in a finite element analysis program which is based on the assumed stress hybrid element and the viscoplasticity-theory.

1. INTRODUCTION

For time-independent elastic-plastic behaviors a very convenient model to represent kinematic hardening is to use an assembledge of elastic-perfectly-plastic elements to represent the stress-strain relation which is approximated by a curve with several piecewise linear segments. This model, which has been widely used for numerical analysis of multiaxial elastic-plastic behavior is named mechanical sublayer or overlay models [refs. 3,4,5]. For more general case including three-dimensional solid, the method should perhaps be called mechanical sub element method.

For plane stress problems the corresponding mechanical model is a laminated plate with layers of elastic-perfectly-plastic materials of different yield stresses. Differential equations for the solutions of plane stress elastic-plastic and isotropic stress-strain relations has been obtained for model with two layers, one of which is elastic and the other is elastic-perfectly-plastic [ref. 6]. The

*Work performed under NASA Grant NAG 3-33.

equations are non-linear and for the case of uniaxial loading the resulting strain hardening behavior will not be a straight line. Thus, for a material with uniaxial stress-strain relation approximated by straight line segments, it is, strickly speaking, not possible to obtain exact representation by a mechanical sublayer described above. In Ref. 6, a relationship has been obtained between the ratio of the initial tangant modulus and the elastic modulus and the thickness ratio of the two layers. It is however, reasonable to assume that by using sufficiently small segments a piecewise linear model can be adopted.

Hunsakier et al. [ref. 5] have also obtained a corresponding relationship for three-dimensional isotropic solids. In that case, for a material represented by one elastic subelement and one elastic-plastic subelement, the resulting uniaxial stress-strain relation will have linear strain hardening behavior. The proportion of the volume of the elastic-plastic element to the total volume V_1/V is expressed simply as

$$\frac{V_1}{V} = \frac{E_1 - E_2}{E_1 - \frac{1-2\nu}{3} E_2}$$

where E_1 is the elastic modulus and E_2, the tangent modulus. In this case, when the uniaxial stress-strain relation is represented by linear segments a corresponding subelement model can be constructed exactly.

The present paper is to extend the mechanical sublayer model to materials with anisotropic plastic behavior. Again the plane stress problem is considered. Finite element method for elastic-plastic analysis based on the viscoplasticity theory and the stress hybrid model is used in conjunction with the present mechanical subelement model. An example solution of a time-independent elastic-plastic problem is presented.

Acknowledgement - The author acknowledges the assistance of Ms. Susan E. French and Mr. Hely Savio for obtaining the numerical results.

2. Mechanical Sublayer Model for Anisotropic Plasticity Problems

Figure 1 is a plate with two layers under plane stress loading. Layer 1 is elastic-perfectly-plastic and is considered tranversely isotropic with yield stresses Y_x and Y_y respectively along the longitudinal and transverse directions. Layer 2 is elastic. The elastic constants E and Poisson's ratio ν for both layers are identical. The yield condition for layer 1 is governed by the Hill's generalized yield criterion

$$f = [F(\sigma_{x_1}-\sigma_{y_1})^2 + G(\sigma_{y_1}-\sigma_{z_1})^2 + H(\sigma_{z_1}-\sigma_{x_1})^2 + K\,\sigma_{xy_1}^2]^{1/2} - \bar{\sigma} = 0 \qquad (1)$$

where $\bar{\sigma} = Y_x$ under uniaxial loading along x direction. With yield stresses under uniaxial loading along y and z direction equal to Y_y, we can express the constants F, H etc. in terms of the yield stresses and obtain the following yield conditions for the plane stress problem

$$f = [\sigma_{x_1}^2 - \sigma_{x_1}\sigma_{y_1} + \alpha\,\sigma_{y_1}^2 + \alpha_s\,\sigma_{xy_1}^2]^{1/2} - Y_x = 0 \qquad (2)$$

where

$$\alpha = (Y_x/Y_y)^2$$
$$\alpha_s = (Y_x/Y_{xy})^2 \qquad (3)$$

The flow rule is

$$\dot{\varepsilon}^p_{x_1} = (\sigma_{x_1} - \tfrac{1}{2}\,\sigma_{y_1})\,\dot{\lambda}$$
$$\dot{\varepsilon}^p_{y_1} = (\alpha\,\sigma_{y_1} - \tfrac{1}{2}\,\sigma_{x_1})\,\dot{\lambda} \qquad (4)$$
$$\dot{\varepsilon}^p_{xy_1} = \alpha_s\,\sigma_{xy_1}$$

Now, consider the behavior of the laminated plate under inplane loading conditions. From testing tension coupons cut along the x and y directions, the elastic modulus for both direction is given as E_1 while the initial tangent moduli are represented, respectively, by E_{x_2} and E_{y_2} as shown in Figure 2. Let σ_x and σ_y represent the average in-plane stresses, then the stress rate σ_y is

$$\dot{\sigma}_y = \dot{\sigma}_{y_1} \frac{t_1}{t} + \dot{\sigma}_{y_2} \frac{t_2}{t} = 0 \tag{5}$$

where t is the total thickness and t_1 and t_2 are the individual thickness. The thickness ratio then is,

$$\frac{t_1}{t_2} = - \frac{\dot{\sigma}_{y_2}}{\dot{\sigma}_{y_1}} \tag{6}$$

Here, layer 2 is elastic hence,

$$\dot{\sigma}_{y_2} = \frac{E_1}{1-\nu^2} (\dot{\varepsilon}_y + \nu \dot{\varepsilon}_x) \tag{7}$$

From $\dot{f} = 0$, we obtain,

$$\dot{\sigma}_{x_1} (2 \sigma_{x_1} - \sigma_{y_1}) + \dot{\sigma}_{y_1} (2\alpha\sigma_{y_1} = \sigma_{x_1}) = 0 \tag{8}$$

Thus, at initial yield when $\sigma_y = \sigma_{y_1} = \sigma_{y_2} = 0$

$$\frac{\dot{\sigma}_{y_1}}{\dot{\sigma}_{x_1}} = 2 \tag{9}$$

and from Eq. (4),

$$\dot{\varepsilon}_{x_1}^{p} = -2\dot{\varepsilon}_{y_1}^{p} \tag{10}$$

We also have

$$\dot{\varepsilon}_{x_1}^{p} = \dot{\varepsilon}_x - \frac{1}{E_1} (\dot{\sigma}_{x_1} - \nu \dot{\sigma}_{y_1}) \tag{11}$$

and $$\dot{\varepsilon}_{y_1}^{p} = \dot{\varepsilon}_y - \frac{1}{E_1}(\dot{\sigma}_{y_1} - \nu \dot{\sigma}_{x_1}) \tag{12}$$

From Eqs. (9) to (12), we obtain,

$$\dot{\sigma}_{x_1} = \frac{E_1}{5 - 4\nu}(\dot{\varepsilon}_x + 2\ \dot{\varepsilon}_y) \tag{13}$$

$$\dot{\sigma}_{y_1} = \frac{E_1}{5 - 4\nu}(2\dot{\varepsilon}_x + 4\ \dot{\varepsilon}_y) \tag{14}$$

Now from the given uniaxial loading conditions the strain rate along y is given by

$$\dot{\varepsilon}_y = \dot{\varepsilon}_y^{e} + \dot{\varepsilon}_y^{p}$$

$$= -\nu\ \dot{\varepsilon}_x^{e} - \frac{1}{2}\dot{\varepsilon}_x^{p} \tag{15}$$

Substituting $$\dot{\varepsilon}_x^{p} = \dot{\varepsilon}_x - \dot{\varepsilon}_x^{e} \tag{16}$$

and $$\dot{\varepsilon}_x^{e} = \frac{\dot{\sigma}_x}{E_1} = \frac{\dot{\varepsilon}_x E_{x_2}}{E_1} \tag{17}$$

into Eq. (15) we obtain

$$\dot{\varepsilon}_y = \dot{\varepsilon}_x \left[-\frac{1}{2} + \left(\frac{1}{2} - \nu\right)\frac{E_{x_2}}{E_1}\right] \tag{18}$$

Substituting into Eqs. (7) and (14) and then into Eq. (16), the following thickness ratio is obtained,

$$\frac{t_1}{t_2} = \frac{5 - 4\nu}{4\ (1 - \nu^2)}\left(\frac{E_1}{E_{x_2}} - 1\right) \tag{19}$$

From which

$$\frac{t_1}{t} = \frac{t_1}{t_1 + t_2} = \frac{E_1 - E_{x_2}}{E_1 - \beta\ E_{x_2}} \tag{20}$$

where

$$\beta = \frac{(1 - 2\nu)^2}{5 - 4\nu} \tag{21}$$

It is noted that this factor β is the same for isotropic materials for which Eqs. (9) and (10) hold. For one dimensional problem the ratio of the area of plastic element to the total area is

$$\frac{A_1}{A} = \frac{E_1 - E_2}{E_1} \tag{22}$$

Thus β is the modification factor for plane stress problems. For $\nu = 0.3$, of Eq. (22) $\beta = (1-2\nu)^2/(5 - 4\nu) = 0.0421$. Thus, the modification is very small when the uniaxial behavior along the longitudinal direction is used to determine the thickness ratio.

Now if a coupon is cut along the y-axis, then when $\sigma_x = \sigma_{x_1} = \sigma_{x_2} = 0$,

$$\frac{\dot{\sigma}_{x_1}}{\dot{\sigma}_{y_1}} = 2\alpha \tag{23}$$

and

$$\dot{\varepsilon}_{y_1}^{p} = -2\alpha\, \dot{\varepsilon}_{x_1}^{p} \tag{24}$$

Following the same derivation given above, if the tangent modulus is E_{y_2}, the thickness ratio becomes

$$\frac{t_1}{t} = \frac{E_1 - E_{y_2}}{E_1 - \beta' E_{y_2}} \tag{25}$$

where

$$\beta' = \frac{(1 - 2\alpha\,\nu)^2}{1 - 4\nu\alpha + 4\alpha^2} \tag{26}$$

For $\nu = 0.3$ and for α between 0.5 and 2, the values of β' is in the range of 0 to 0.35.

Equating Eqs. (19) and (26) and solving for E_1' we obtain a relation between E_{x_2} and E_{y_2},

$$E_{y_2} = \frac{(1 - \beta)\, E_1\, E_{x_2}}{(1 - \beta')\, E_1 - (\beta - \beta')\, E_{x_2}} \tag{27}$$

Thus for anisotropic material represented by the mechanical sublayer model the initial tangent moduli for the two directions are not the same. When the stress-strain curves for two perpendicular directions are given, a mechanical sublayer can be obtained according to the following procedure.

(1) For the stress-strain curves, for both x-and y-direction determine the initial yield stresses Y'_{x_1} and Y'_{y_1}. These are also the yield stresses Y_{x_1} and Y_{y_1} of the sublayer and are euqal to $E_1 \varepsilon_{x_1}$ and $E_1 \varepsilon_{y_1}$, respectively.

(2) Based on one of the curves say for the x direction try an initial tangent modulus E_{x_2}. Knowing Y_{x_1}, Y_{y_1}, and E_{x_2}, α and β for layer 1 can be determined, hence, t_1/t can be calculated from Eq. (2) and the initial tangent modulus E_{y_2} for the y-direction, from Eq. (27).

(3) The 2-sublayer model is then used to analyze two uniaxial loading problems and to obtain the stress-strain curves for both directions. The intersections of these lines to the actual stress-strain curves now determines the second set of transition points at which the second layer yields. The stresses and strains are respectively Y'_{x_2} and Y'_{y_2} and ε_{x_2} and ε_{y_2} as shown in Figure 3. In general, the yield stresses Y_{x_2} and Y_{y_2} of the new sublayer are not equal to $E_1 \varepsilon_{x_2}$ and $E_1 \varepsilon_{y_2}$, although in the case of subelement model for uniaxial problems, the yield stress for the second subelement is equal to $E_1\varepsilon_2$.

For 3-D problems with isotropic plastic behavior, Hunsaker has obtained closed form solutions for the case of a 2-subelement model. For a typical case with $E_2 = 0.5\ E_1$ and $\varepsilon_2 = 3\ \varepsilon_1$ the difference between Y'_2 and $E_1\ \varepsilon_2$ is only 5%.

The choice of the initial tangent modulus E_{x_2} must be such that the second set of transition points do fall on the actual stress-strain curve. In general, an iterative procedure is required.

(4) The plate is now considered as a new two-layer model with the yield stresses for the two directions equal to Y_{x_2} and Y_{y_2}. Then by choosing a tangent modulus E_{x_3} for the next segment, values of $(t_1 + t_2)/t$, E_{y_3}, and Y_{x_3}, Y_{y_3}, Y_{x_3}, and Y_{y_3} can be determined following the same steps (2) and (3) above using

$$\frac{t_1 + t_2}{t} = \frac{E_1 - E_{x_3}}{E_1 - \beta E_{x_3}} \tag{28}$$

and

$$E_{y_3} = \frac{(1 - \beta) E_1 E_{x_3}}{(1 - \beta') E_1 - (\beta - \beta') E_{x_3}} \tag{29}$$

for the value of β' Eq. (26) is used with $\alpha = (Y_{x_2}/Y_{y_2})^2$.

(5) The mechanical sublayer model may be constructed using the stress-strain curve for the transverse direction as reference. In that case, Eq. (25) as used to determine the thickness ratio's and Eq. (27) is used to solve for E_{x_i} in terms of E_{y_i}.

In the solution of a plane stress problem given in this paper a simplified procedure was adopted. The stress-strain curves for either the longitudinal or the transverse directions is replaced by a curve with linear segments. With one of the tangent moduli given, the other tangent modulus can be obtained and is again considered constant. Thus, the intercept of this linear segment to the actual stress-strain curve can be determined. The yield stresses for sublayers are obtained by the simple formulas,

$$Y_{x_i} = E_1 \varepsilon_{x_i} \tag{30}$$

and

$$Y_{y_i} = E_1 \varepsilon_{y_i}$$

3. Finite Element Method Based on Viscoplasticity Theory

Time independent elastic-plastic analysis can be made by using viscoplasticity models [ref. 7]. In the case of elastic-perfectly-plastic material, it is only necessary to consider the rate of viscoplastic strain components ε^{vp} as

$$\dot{\varepsilon}^{vp} = \gamma < \phi > \frac{\partial F}{\partial \underset{\sim}{\sigma}} \tag{31}$$

where $F(\underset{\sim}{\sigma}) = 0$ represents the yield surface and

$$< \phi > = \begin{cases} \bar{\sigma} - \sigma_y & \text{for } \sigma > \sigma_y \\ 0 & \text{for } \sigma \leq \sigma_y \end{cases} \tag{32}$$

$\bar{\sigma}$ = equivalent stress

σ_y = yield stress under uniaxial loading

γ = a fluidity parameter which is arbitrary for the corresponding elastic-plastic analysis.

A corresponding viscoplastic model for the mechanical sublayer model is an arrangement of viscoplastic elements in parallel as shown in Figure 4.

In the finite element analysis of a plane stress problem, the entire panel is discretized into N finite elements, the thickness of each of which is divided into M sublayers according to the modelling described in the previous section. A finite element method for the creep problem has been formulated by the initial strain approach using the assumed stress hybrid model [8,9]. The method is extended to the present multilayer model. For the incremental solution of the elastic-plastic problem, the procedure is as follows,

(1) An elastic solution of nodal displacements due to a given load increment is made using the assumed stress hybrid elements,

(2) The stress increments at selected Gaussian stations in each element are evaluated,

(3) The stresses in each sublayer at each Gaussian station are updated and the corresponding equivalent stress $\bar{\sigma}$ evaluated,

(4) A time increment Δt is chosen and the increments of viscoplastic strains are $\Delta \underset{\sim}{\varepsilon}^{vp} = \dot{\underset{\sim}{\varepsilon}}^{vp} \Delta t$ for all sublayers at all Gaussian stations. Here the viscoplastic strain rates are determined by Eqs. (31) and (32).

(5) The equivalent nodal forces due to the viscoplastic strain increments can be evaluated. They are used for the determination of nodal displacements for the time increment.

(6) Steps (2) and (5) are repeated until the changes in stresses within the time increment become less than a small prescribed limit.

At this stage, the equivalent stress $\bar{\sigma}$ in each sublayer is either equal or smaller than the yield stress of that sublayer and stabilized stress state for this loading increment is obtained. The use of successive time increments is equivalent to an iterative procedure for this elastic-plastic problem.

A guideline for the choice of the time increment Δt to assure numerical stability is, according to Cormeau [ref. 10],

$$\Delta t \leq \frac{4\ (1+\nu)}{3\ E\ \gamma} \tag{33}$$

where E is the Young's modulus

4. Anisotropic Analysis of Shear Lag Structure

To illustrate the finite element solution using the present anisotropic model, a shear lag structure which was tested in 1963 at Massachusetts Institute of Technology is used [ref. 11]. The structure shown in Figure 5 was integrally

machined from thick 2024-T4 aluminum alloy plate. It is a rectangular panel 27.94 cm x 25.4 cm x .203 cm, stiffened by tapered stiffners along the loading (y) axis. The stiffness became flush with the panel at the center, where the stresses and strains are the highest under the applied tension load through the stiffners.

Fitted stress-strain curves for both the longitudinal or x-direction and the transverse or y-direction were obtained from tension tests as shown in Figure 6. An average of these two curves is also shown.

A mechanical sublayer model for this material was constructed by the simplified procedure indicated in section 2. The corresponding curves with piecewise linear senments are shown in Figure 7. The yield stress under shear was not obtained in the original experiment. For the mechanical sublayer model, the values of Y_{xy} for each layer is set equal to $Y/\sqrt{3}$ where Y is the larger of Y_x and Y_y. Of the five sublayers used in the models the last one is considered elastic. The strain disbribution of the panel, thus, is determined directly by the elastic strains of this layer. Table 1 lists the thickness ratios and yield stresses of the various sublayers.

For the finite element analysis one quarter of the panel is used. It is subdivided into 7 x 7 rectangular plane stress elements as shown in Figure 8. The tapered stiffness is also modelled as plane stress elements with constant thickness in each element. For the finite element solution all numerical integrations were obtained by using 2 x 2 Gaussian quadrature.

The resulting strains ε_x and ε_y at the center of the panel were determined by extrapolating from the two Gaussian stations along the diagonal line of the element at closest to the center. Their variations with respect to the applied load are shown in Figure 9. Also plotted for comparison are:

(1) A finite element solution obtained by the present method but by modelling as an isotropic material based on the average stress-strain curve shown in Figure 6.

(2) A finite element solution obtained by Jensen et al. [ref. 12], using 144 constant strains triangular elements and by modelling as an isotropic material.

(3) Experimental results obtained in Ref. 11.

It is seen that the solutions by the three finite analyses are comparable although they do not agree with the experimental result, especially, for the ε_y component. In this particular case the approximate solution obtained by considering the material property to isotropic appears to be very close to that by the present modelling of anisotropic material.

5. Conclusions

A method has been developed for the modelling of anisotropic plastic behaviors for metals by the mechanical subelement model. It has been incorporated in a finite element analysis program based on the assumed stress hybrid model and, on the viscoplasticity theory.

REFERENCES

1. P. Duwez, "On the Plasticity of Crystals," Physical Review, 47, 494-501, 1935.

2. J. F. Besseling, "A Theory of Plastic-flow for Anisotropic Hardening in Plastic Deformation of an Initially Isotropic Material," Nat. Aero Research Inst. Rept. S410, Amsterdam, 1953.

3. J. W. Leech, E. A. Witmer and T. H. H. Pian, "Numerical Calculation Technique for Large Elastic-Plastic Transient Deformations of Thin Shells," AIAA Journal 6, 2352-2359, 1968.

4. O. Z. Zienkiewicz, G. C. Nayak and D. R. J. Owen, "Composite and Overlay Models in Numerical Analysis of Elastic-Plastic Continua," Foundations of Plasticity, A. Sawszuk ed. Noordhoff, Leyden, 107-123, 1973.

5. B. Hunsaker, W. E. Haisler and J. A. Stricklin, "On the Use of Two Hardening Rules of Plasticity in Incremental and Pseudo Force Analyses," Constitutive Equation's in Viscoplasticity: Computational and Engineering Aspect, ASME, AMD-Vol. 20, 139-170, 1973.

6. T. H. H. Pian, Unpublished lecture notes on Plasticity, 1966.

7. P. Perzyna, "Fundamental Problems in Viscoplasticity," Advances in Applied Mechanics," Academic Press, New York, Vol. 9, 243-377, 1966.

8. T. H. H. Pian, "Nonlinear Creep Analysis by Assumed Stress Finite Element Methods," AIAA Journal, Vol. 12, 1756-1758, 1975.

9. T. H. H. Pian, and S. W. Lee, "Creep and Viscoplastic Analysis by Assumed Stress Hybrid Finite Elements," Finite Elements in Nonlinear Solid and Structural Mechanics, Ed. by P. G. Bergan et al. Tapir Publisher Trondheim, Norway,807-822, 1978.

10. I. C. Cormeau, "Numerical Stability in Quasi-State Elasto/Viscoplasticity," Int. J. Num. Meth. Engng., 9, 109-127, 1975.

11. J. H. Percy, W. A. Loden and D. R. Navaratua, "A Study of Matrix Analysis Methods for Inelastic Structures," Air Force Dynamics Laboratory Report, RTD-TDA-63-4032, Oct. 1963.

12. W. R. Jeusen, W. E. Falby and N. Prince, "Matrix Analysis Methods for Anisotropic Inelastic Structures," Air Force Flight Dynamics Lab. Report AFFDL-TR-65-220, April 1966.

Table 1. Constants for Mechanical Sublayer Model (Anisotropic Plasticity)

Layer Number i	1	2	3	4	5
t_i/t	0.360	0.351	0.130	0.130	0.029
E_{x_i} GPa	69.6	45.2	20.8	11.5	2.08
E_{y_i} GPa	69.6	44.7	20.3	11.2	2.01
ε_{x_i} 10^{-3}	5.01	5.33	5.52	6.01	10.0
ε_{y_i} 10^{-3}	3.24	4.52	6.22	8.44	14.0
Y_{x_i} $(=E_i\varepsilon_{x_i})$ MPa	349	371	385	419	ELASTIC
Y_{y_i} $(=E_i\varepsilon_{y_i})$ MPa	226	315	433	587	
$\alpha_i = (Y_{x_i}/Y_{y_i})^2$	2.39	1.39	0.789	0.508	
$\alpha_{s_i} = (Y_{x_i}/Y_{s_i})^2$	7.17	4.17	3	3	

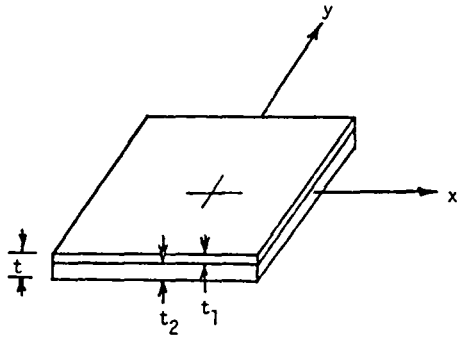

Figure 1. Two-Layer Model Representing Strain Hardening Behavior

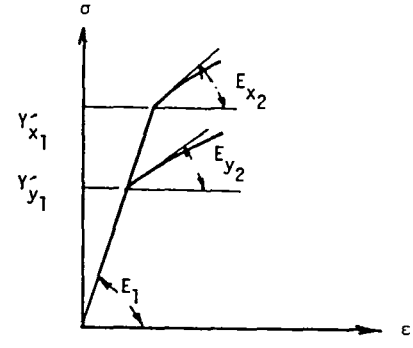

Figure 2. Uniaxial Stress-Strain Relations for Two-Layer Model

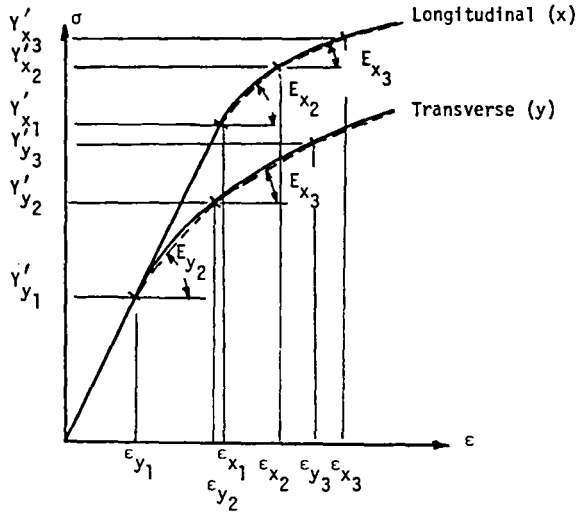

Figure 3. Stress-Strain Relations by Mechanical Sublayer Model

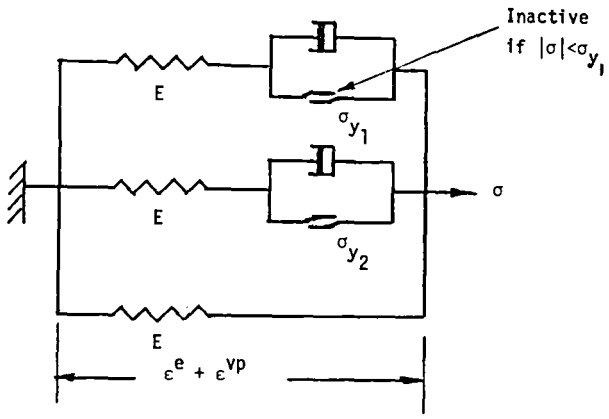

Figure 4. Viscoplastic Model for Mechanical Sublayers

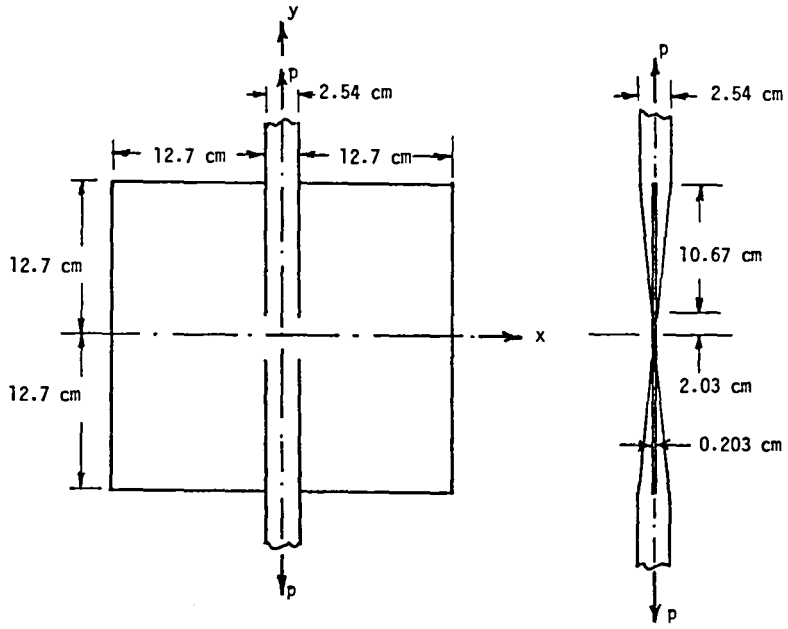

Figure 5. Dimensions of Shear Lag Structure

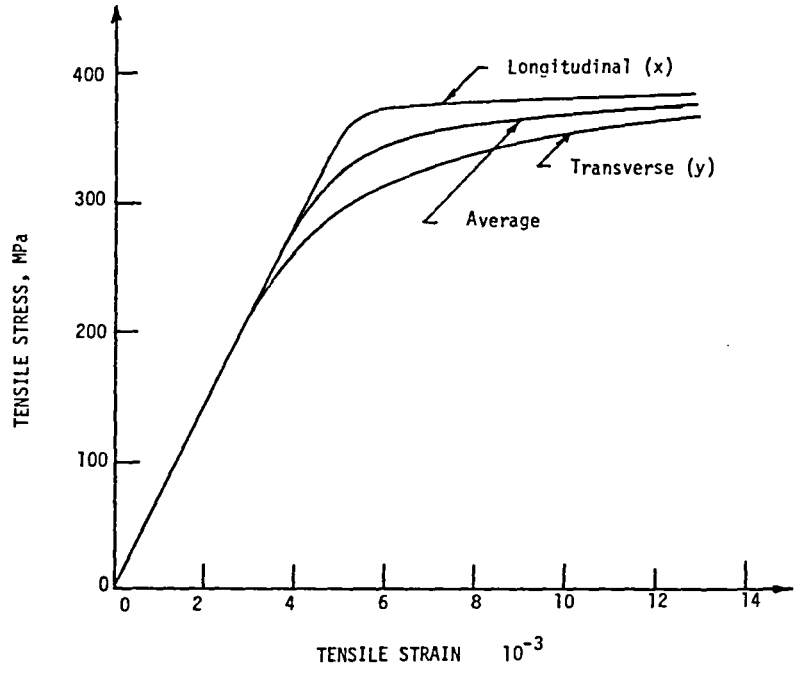

Figure 6. Fitted Stress-Strain Curves of 2024-T4 Aluminum Alloy Plate

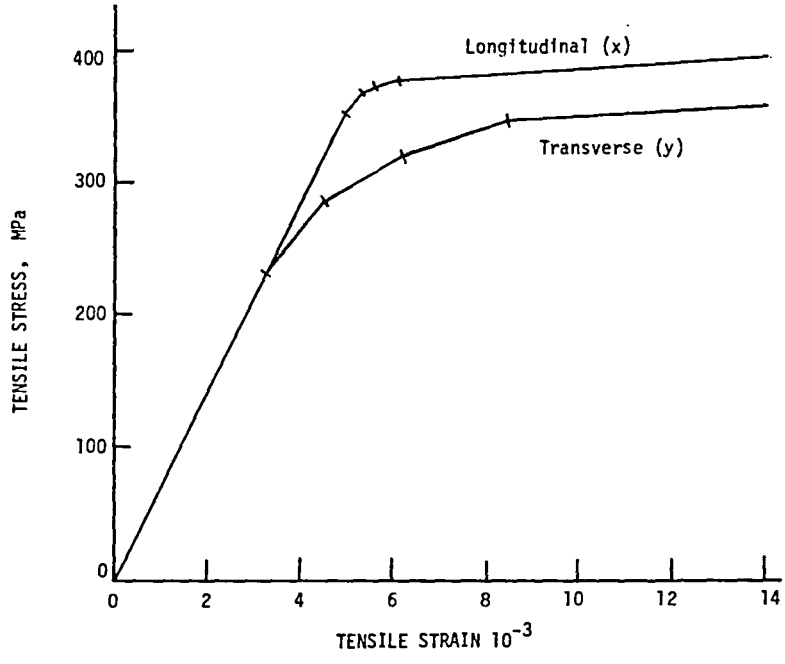

Figure 7. Approximate Stress-Strain Curves by Mechanical Sublayer Model (2024-T4)

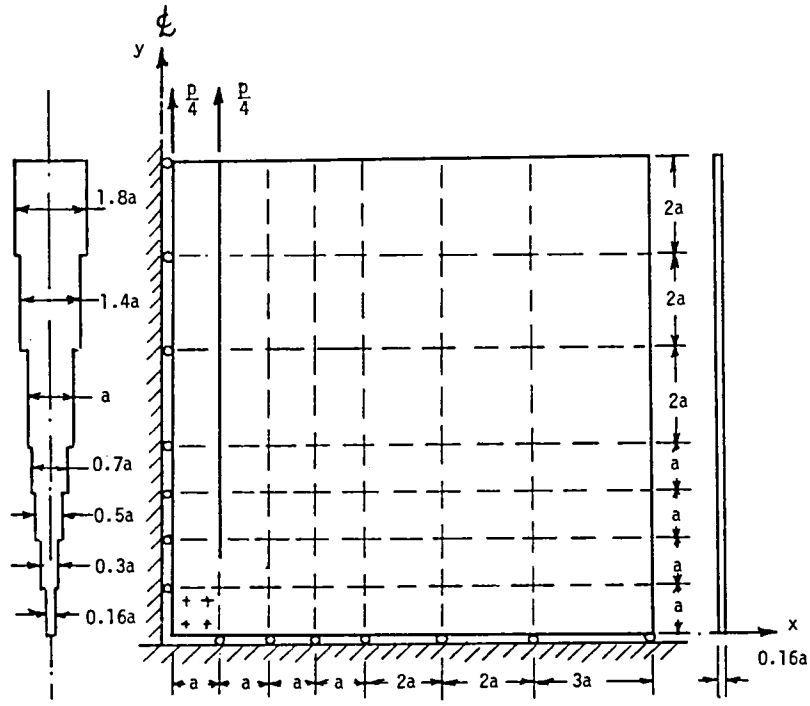

a = 1.27 cm

Figure 8. Finite Element Mesh for Shear Lag Structure

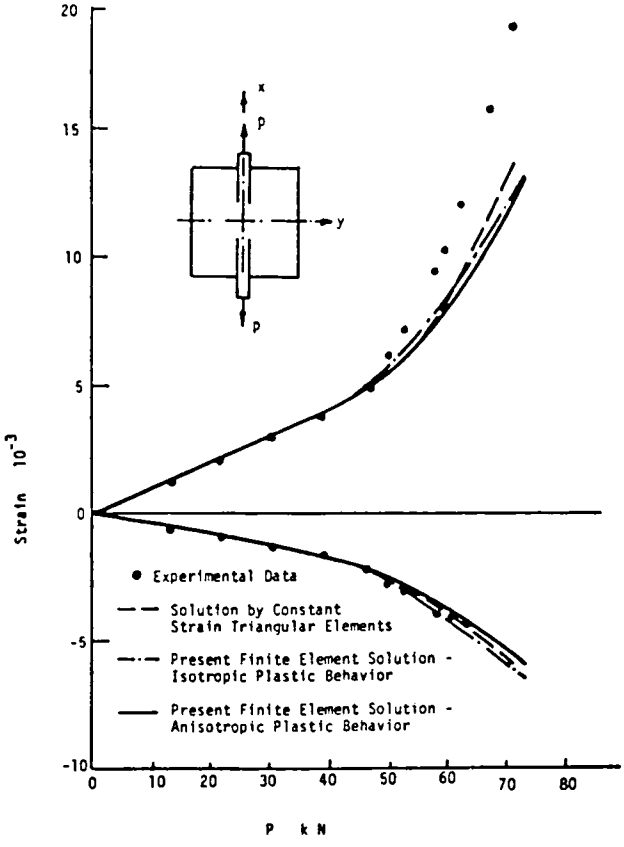

Figure 9. Strain Components at Center of Shear Lag Structure - Comparison of Different Finite Element Solutions